Molecular Biology of the Cell
Vol. 13, 1366–1380, April 2002

Reorientation of Mispositioned Spindles in Short Astral Microtubule Mutant *spc72Δ* Is Dependent on Spindle Pole Body Outer Plaque and Kar3 Motor Protein[V]

Dominic Hoepfner, Florian Schaerer, Arndt Brachat,* Achim Wach,† and Peter Philippsen‡

Lehrstuhl für Angewandte Mikrobiologie, Biozentrum, Universität Basel, CH-4056 Basel, Switzerland

Submitted July 2, 2001; Revised December 10, 2001; Accepted January 14, 2002
Monitoring Editor: Tim Sterns

Nuclear migration and positioning in *Saccharomyces cerevisiae* depend on long astral microtubules emanating from the spindle pole bodies (SPBs). Herein, we show by in vivo fluorescence microscopy that cells lacking Spc72, the SPB receptor of the cytoplasmic γ-tubulin complex, can only generate very short (<1 μm) and unstable astral microtubules. Consequently, nuclear migration to the bud neck and orientation of the anaphase spindle along the mother-bud axis are absent in these cells. However, *SPC72* deletion is not lethal because elongated but misaligned spindles can frequently reorient in mother cells, permitting delayed but otherwise correct nuclear segregation. High-resolution time-lapse sequences revealed that this spindle reorientation was most likely accomplished by cortex interactions of the very short astral microtubules. In addition, a set of double mutants suggested that reorientation was dependent on the SPB outer plaque and the astral microtubule motor function of Kar3 but not Kip2/Kip3/Dhc1, or the cortex components Kar9/Num1. Our observations suggest that Spc72 is required for astral microtubule formation at the SPB half-bridge and for stabilization of astral microtubules at the SPB outer plaque. In addition, our data exclude involvement of Spc72 in spindle formation and elongation functions.

INTRODUCTION

In most eukaryotic organisms the position of the spindle determines the location of the cleavage furrow at cytokinesis (Hyman, 1989). In the budding yeast *Saccharomyces cerevisiae* this is not the case. The plane of cytokinesis is predefined by the position of an emerging bud. To ensure that both the mother and daughter cell receive a nucleus upon spindle elongation, the spindle has to be actively positioned close to the mother-daughter junction (the bud neck) and oriented along the mother-daughter axis.

These processes are accomplished by the action of dynamic forces acting on the nuclei via microtubules (reviewed by Hildebrandt and Hoyt, 2000). Microtubules can be classified as nuclear or astral (cytoplasmic) (Byers and Goetsch, 1975). Nuclear microtubules are involved in assembly of a bipolar spindle and in segregation of the chromosomes (Jacobs *et al.*, 1988; Straight *et al.*, 1997); astral microtubules function to position, move, and orient the spindle and thus the nucleus within the cell (Palmer *et al.*, 1992; Sullivan and Huffaker, 1992; Carminati and Stearns, 1997; Shaw *et al.*, 1997; Tirnauer *et al.*, 1999). All microtubules are organized by the spindle pole body (SPB) the functional homolog of the microtubule organizing center of higher eukaryotic cells. In electron micrographs, the spindle pole body appears as a three-laminar structure embedded in the nuclear envelope and a one-sided extension of the central layer localized on top of the nuclear envelope called a half-bridge (Moens and Rapport, 1971; Byers and Goetsch, 1975).

Microtubules are nucleated on the γ-tubulin complex that consists of Spc98, Spc97, and Tub4 (Geissler *et al.*, 1996; Knop *et al.*, 1997; Murphy *et al.*, 1998, Rout and Kilmartin, 1990). The γ-tubulin complex assembles in the cytoplasm and is then targeted and anchored to the inner plaque of the SPB by Spc110 and to the outer plaque and half-bridge region by Spc72 (Rout and Kilmartin, 1990; Spang *et al.*, 1996; Knop and Schiebel, 1997, 1998; Nguyen *et al.*, 1998). Although the interaction sites of Spc110 with the γ-tubulin complex and the SPB have been identified and its function is relatively

Article published online ahead of print. Mol. Biol. Cell 10.1091/mbc.01–07–0338. Article and publication date are at www.molbiolcell.org/cgi/doi/10.1091/mbc.01–07–0338.

[V] Online version of this article contains video material for some figures. Online version available at www.molbiolcell.org.

Present addresses: *Novartis Oncology, CH-4002 Basel, Switzerland; †Bureco Corporation, CH-4123 Allschwil, Switzerland.

‡ Corresponding author. E-mail address: peter.philippsen@unibas.ch.

Table 1. Yeast strains used in this study

Name	Genotype	Source
FY 1679	*MATa/α ura3-52/ura3-52 trp1Δ63/TRP1 leu2Δ1/LEU2 his3Δ200/HIS3*	B. Dujon
CEN.PK2	*MATa/α ura3-52/ura3-52 trp1-289/trp1-289 leu2-3,112/leu2-3,112 his3Δ1/his3Δ1*	K.D. Entian
DHY6	*MATa/α HHF2::GFP-KanMX6/HHF2 ura3-52Δ1/ura3-52Δ1 trp1Δ63/TRP1 leu2Δ1/LEU2 his3Δ200/HIS3*	This study
DHY19	*MATa/α HHF2::GFP-His3MX6/HHF2 spc72Δ1::KanMX4/spc72::KanMX4 ura3-52/ura3-52 trp1Δ63/TRP1 leu2Δ1/LEU2 his3Δ200/HIS3*	This study
DHY177	*MATa/α spc72Δ1::KanMX4/SPC72 cnm67Δ1::klTRP1/CNM67 ura3-52/ura3-52 trp1-289/trp1-289 leu2-3,112/leu2-3,112 his3Δ1/his3Δ1*	This study
DHY195	*MATα ura3Δ1::GFP-TUB1-URA3(pAFS125) trp1Δ63 LEU2 HIS3*	This study
DHY205	*MATα ura3Δ1::GFP-TUB1-URA3(pAFS125) spc72Δ1::klTRP1 trp1Δ63 LEU2 HIS3*	This study
DHY208	*MATa/α ura3Δ1::GFP-TUB1-URA3(pAFS125)/ura3-52Δ1::GFP-TUB1-URA3(pAFS125) spc72Δ1::klTRP1/spc72Δ1::KanMX4 trp1Δ63/trp1Δ63 leu2Δ1/LEU2 his3Δ200/his3Δ200*	This study
DHY209	*MATa/α ura3Δ1::GFP-TUB1-URA3(pAFS125)/ura3-52Δ1::GFP-TUB1-URA3(pAFS125) trp1Δ63/TRP1 LEU2/LEU2 his3Δ200/HIS3*	This study
DHY236	*MATa/α spc72Δ1::klTRP1/SPC72 kip2Δ1::KanMX4/KIP2 ura3-52/ura3-52 trp1-289/trp1-289 leu2-3,112/leu2-3,112 his3Δ1/his3Δ1*	This study
DHY237	*MATa/α spc72Δ1::klTRP1/SPC72 kip3Δ1::KanMX4/KIP3 ura3-52/ura3-52 trp1-289/trp1-289 leu2-3,112/leu2-3,112 his3Δ1/his3Δ*	This study
DHY238	*MATa/α spc72Δ1::klTRP1/SPC72 kar3Δ1::KanMX4/KAR3 ura3-52/ura3-52 trp1-289/trp1-289 leu2-3,112/leu2-3,112 his3Δ1/his3Δ*	This study
DHY239	*MATa/α spc72Δ1::klTRP1/SPC72 num1Δ1::KanMX4/NUM1 ura3-52/ura3-52 trp1-289/trp1-289 leu2-3,112/leu2-3,112 his3Δ1/his3Δ*	This study
DHY242	*MATa/α spc72Δ1::klTRP1/SPC72 Δhc1Δ1::KanMX4/ΔHCl ura3-52/ura3-52 trp1-289/trp1-289 leu2-3,112/leu2-3,112 his3Δ1/his3Δ1*	This study
DHY259	*MATα kar3Δ1::KanMX4 ura3Δ1::GFP-TUB1-URA3(pAFS125) trp1-289 leu2-3,112 his3Δ1*	This study
DHY278	*MATα spc72Δ1::klTRP1 ura3Δ1::GFP-TUB1-URA3(pAFS125) trp1-289 leu2-3,112::pspc72-7-LEU2 his3Δ1*	This study
DHY280	*MATa spc72Δ1::klTRP1 kar3Δ1::KanMX4 ura3Δ1::GFP-TUB1-URA3(pAFS125) trp1-289 leu2-3,112::pspc72-7-LEU2 his3Δ1*	This study
DHY282	*MATa/α spc72Δ1::klTRP1/SPC72 kar9Δ1::KanMX4/KAR9 ura3-52/ura3-52 trp1-289/trp1-289 leu2-3,112/leu2-3,112 his31/his3Δ*	This study
DHY293	*MATα cnm67Δ1::His3MX6 ura3-52 trp1-289 leu2-3,112 his3Δ1*	This study
DHY317	*MATα spc72Δ1::klTRP1 cnm67Δ1::His3MX6 ura3Δ1::GFP-TUB1-URA3(pAFS125) trp1-289 leu2-3,112::pspc72-7-LEU2 his3Δ1*	This study

well understood (Kilmartin and Goh, 1996; Knop and Schiebel, 1997; Nguyen *et al.*, 1998), the function of Spc72 remains less clear. The observations that astral microtubules are localized to two different cytoplasmic SPB substructures during specific phases of the cell cycle, the outer plaque and the half-bridge, and that Spc72 is present at both substructures suggest that Spc72 may have multiple functions.

Nuclear segregation and thus cell viability have been shown to be strictly dependent on intact astral microtubules (Sullivan and Huffaker, 1992). Based on the proposed function of Spc72 as an anchor of the γ-tubulin complex and thus the site for astral microtubule formation, loss of Spc72 was expected to result in a lethal phenotype (Chen *et al.*, 1998; Knop and Schiebel, 1998). This however was not the case in several strain backgrounds (Souès and Adams, 1998; this study). Remarkably, cells lacking Spc72 displayed defects in astral microtubule formation and in nuclear segregation, yet still were able to proliferate. This raises the question how cells with impaired or even absent astral microtubules position their spindles and segregate their nuclei?

In this study, we describe live cell imaging of green fluorescent protein (GFP)-labeled nuclei and microtubules in wild-type and *spc72Δ* deletion mutants. Our observations enable us to propose a model that explains the nuclear dynamics defect observed in cells lacking Spc72 and also how residual successful nuclear segregation occurs in the absence of Spc72 protein. Phenotypes of various double mutants supported the observations of the time-lapse studies and revealed an astral microtubule motor essential for cell viability in the absence of the Spc72 protein. In addition, our data exclude involvement of Spc72 in nuclear spindle functions. Finally, our results are the first dynamic analyses of cells lacking the Spc72 protein and together with data of previous studies provide a new, more coherent image of Spc72 function.

MATERIALS AND METHODS

Strains, Media, and Yeast Transformation

Yeast strains used in this study are summarized in Table 1. Yeast media were prepared as described by Guthrie and Fink (1991). The yeast transformation procedure was based on the protocol by Schiestl and Gietz (1989). After the heat shock step, cells were pelleted and resuspended in 5 ml of YPD and incubated for 2 h at 30°C. Cells were again pelleted, resuspended in 1 ml of distilled H_2O, and plated on selective YPD-G418 medium (200 mg/l geneticin). The *Escherichia coli* strain XL1-blue (Bullock *et al.*, 1987) was used to propagate plasmids.

DNA Manipulations and Strain Constructions

Standard DNA manipulations were performed as described by Sambrook *et al.* (1989). We applied a polymerase chain reaction (PCR)-based method to construct gene deletion cassettes that were used in yeast transformations (Wach *et al.*, 1994). DNA of *E. coli* plasmids pFA6-KanMX4 (Wach *et al.*, 1994), pFA6-HIS3MX6, pFA6-GFP-KanMX6, pFA6-GFP-HIS3MX6 (Wach *et al.*, 1997), and pYM3-klTRP1 (Knop *et al.*, 1999) served as the template for preparative PCR reactions. Correct genomic integration of the corresponding construct was verified by analytical PCR (Huxley *et al.*, 1990; Wach *et al.*, 1994). Yeast strains were grown on YPD-G418 (200 mg/l geneticin) to select for transformants that had integrated KanMX4, or GFP-KanMX6 cassettes. SD plates lacking histidine or tryptophane were used to select for GFP-HIS3MX6, HIS3MX6, or klTRP1 integration.

For gene deletions we followed the EUROFAN guidelines (Wach, Brachat, and Philippsen [1996], Guidelines for EUROFAN B0 program ORF deletants, plasmid tools, basic functional analyses, available at www.mips.biochem.mpg.de/proj/eurofan/index.html) for gene replacement in *S. cerevisiae*. We used the following oligonucleotide pairs for generation of the KanMX4, His3MX6, klTRP1 deletion cassettes with flanking homologies to the target genes: *spc72Δ1*: 5′-A A C A C T A A T A T C A A A A A A C T A A G C A A A C A A C A T A A G G A A A G T T A T A G C C G C T T C G T A C G C T G C A G G T C G-3′ and 5′-A G A G T G A C T G A G T G T T A C A T T A A A T A T A T T T A T A T A T A A A C G T A T G A T A T A T C A T C G A T G A A T T C G A G C T C G T T-3′ The oligonucleotide pairs used for deletion of *KIP2*, *KIP3*, *KAR3*, *DHC1*, *KAR9*, *NUM1*, and *CNM67* are described by Hoepfner *et al.* (2000). C-Terminal fusion of the S65T variant of GFP to Hhf2 (histone H4) was performed as described by Wach *et al.* (1997). This label was used in one copy in diploid strains. Growth rate and morphology of these strains were indistinguishable from those of wild type. To label microtubules we integrated plasmid pAFS125 into the *ura3* locus (Straight *et al.*, 1997). Spindle and astral microtubules were clearly observable under the fluorescence microscope upon successful transformation. The suitability of this label for in vivo studies has already been demonstrated (Straight *et al.*, 1997). SPC72 temperature-sensitive (ts) mutants were generated by integrating the linearized *pspc72-7* plasmid (Knop and Schiebel, 1998) into the *leu2* locus of cells deleted for *SPC72*. Generation of double mutants was achieved either by crossing of the single mutants followed by sporulation and dissection of the four-spored asci or by serial gene deletion with the kanMX4/His3MX6 and the klTRP1 cassette.

In Vivo Microscopy Procedures and Techniques

The video microscopy setup and in vivo time-lapse procedures with Hhf2-GFP– or GFP-Tub1–labeled strains were described by Hoepfner *et al.* (2000). We preferentially used diploid cells because spreading of the cells during the time-lapse experiment was better due to the bipolar budding pattern. Haploid cells overgrew each other rapidly impairing long observation of individual cells. General Hhf2-GFP acquisition settings were as follows: 1-min interval time, 0.1-s exposure time, 3% illumination transmission, one *z*-axis plane, and no binning. General GFP-Tub1 acquisition settings were as follows: 2-min interval time, 0.4-s exposure time, 50% illumination transmission, three *z*-axis planes spaced by 0.8 μm, and 2×2 binning. By using these conditions cells showed steady growth for up to 72 h. Nuclear and microtubule dynamics of individual cells could be tracked for more than eight divisions. Acquisition settings for the high-resolution GFP-tub1 studies were as follows: 15-s interval time, 1-s exposure time, 100% illumination transmission, three *z*-axis planes spaced by 0.8 μm, and no binning. The temperature of immersion oil on the microscope slide near the sample was ~24°C. The *z*-axis stacks were merged into one plane by using the "stack arithmetic:maximum" command of MetaMorph. The stored images were then scaled and converted to 8-bit files. A red look-up table was assigned to the phase-contrast image, and a green look-up table was assigned for the fluorescence image. The phase-contrast and fluorescence 8-bit planes were then overlaid using the built-in "overlay" command with the default balance. For time-lapse analysis we then assembled the picture files to a movie in QuickTime format (Apple Computer, Cupertino, CA) with frame rate of 10 frames/s by using the Premiere 4.2 program (Adobe Systems Europe, Edinburgh, Scotland).

Acquisition of Still Images

GFP-Tub1–engineered wild-type and *spc72*Δ strains were grown in YPD medium to early log phase at 30°C. Three microliters of the culture was spread on a poly-L-lysine–treated slide overlaid with a coverslip, sealed with nail polish, and immediately used for microscopy. No prepared slide older than 5 min was analyzed. GFP-Tub1–engineered *spc72-7* stains were grown at 23°C to early log phase and analyzed as described above. To analyze the phenotype at the nonpermissive temperature, early log phase cultures were shifted from 23 to 37°C for 3 h then 3 μl of culture was spread on a 37°C prewarmed, poly-L-lysine–treated slide and immediately used for microscopy. The microscope stage was temperature adjustable and set to 37°C. No prepared slide older than 5 min was analyzed. Acquisition settings were as follows: 1-s exposure time, 100% illumination transmission, five *z*-axis planes spaced by 0.8 μm, and no binning. Images were processed as described by Hoepfner *et al.* (2000).

RESULTS

Impaired Nuclear Positioning and Spindle Orientation in spc72Δ Cells

We analyzed nuclear dynamics in diploid wild-type (Movie 1A) and *spc72*Δ (Movie 1B) cells by in vivo time-lapse fluorescence microscopy. These cells expressed green fluorescent protein-tagged histone H4 (Hhf2-GFP), which was shown in previous studies to mark nuclei in *S. cerevisiae* without interfering with the nuclear cycle (Wach *et al.*, 1997; Hoepfner *et al.*, 2000). In contrast to wild type we observed an accumulation of bi- and multinucleate as well as anucleate cells in microcolonies of the *spc72*Δ mutant (Movie 1B; representative frames shown in Figure 1). To investigate the basis for this frequent failure in segregation of daughter nuclei we at first analyzed the behavior of nuclei in early steps of 220 cell cycles. In particular, we monitored nuclear positioning (movement of the nucleus to the bud neck before anaphase), nuclear orientation (alignment of the elongating nucleus along the mother-bud axis, mirroring spindle orientation), and insertion of the anaphase nucleus into the bud neck (mirroring spindle insertion) in *spc72*Δ cells carrying a single nucleus. Mutant cells with more nuclei will be discussed in a later section.

Nuclear oscillations and movements typical for the G1 phase of wild-type cells (Movie 1A) were completely absent in s*pc72*Δ mutants (Movie 1B). Occasional movements of the nucleus were only observed when the vacuole (sometimes visible in the red phase-contrast image of Movie 1B) displaced the nucleus. The nucleus normally did not move from the position at which it had been placed at the end of the previous cell cycle. A quantitative evaluation revealed that only 24% of *spc72*Δ cells had preanaphase nuclei positioned close to the bud neck (Table 2), not due to active movement of the nucleus toward the nascent bud, but rather due to the fact that these nuclei where positioned by chance at this site during the previous mitosis.

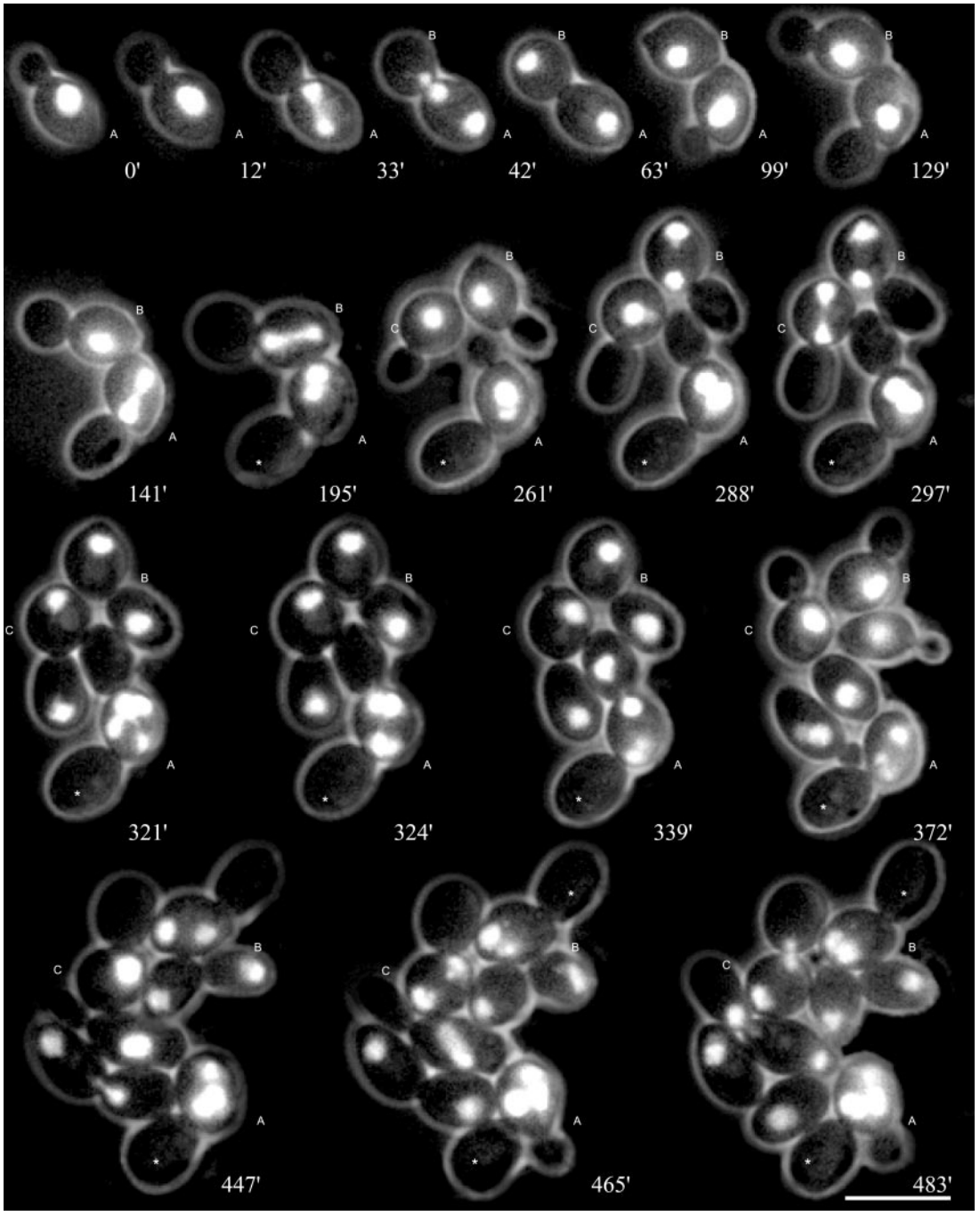

Figure 1. Nuclear migration dynamics of diploid *spc72*Δ cells. Mitotic cell cycles were observed by in vivo time-lapse fluorescence microscopy for several generations. Representative frames of Movie 1B are presented. Compared with wild-type cells, shown in Movie 1A, the following differences can be seen. Nuclear positioning of the preanaphase nucleus to the bud-neck is absent (e.g., 0′, cell A), spindle elongation during anaphase is restricted to the mother cell and elongation of the anaphase spindle does frequently not occur along the mother-bud axis (33′, cell A). Nevertheless, delayed but successful segregation of one of the daughter nuclei into the bud is often observed (42′–63′, cell A). On the other hand, even correct spindle alignment (141′, cell A) is sometimes followed by a failure in nuclear segregation, leading to a binucleate mother cell and an anucleate bud. (195′–297′, cell A). Nuclear divisions in binucleate cells occur simultaneously (321′, cell A). After successful transit of a nucleus into the bud, cell separation can be observed by a change of the position of the bud relative to the mother cell after cytokinesis (63′–99′, cell A). Anucleate buds (marked with asterisks) are not separated from the mother cell during subsequent cell cycles. Bar, 10 μm. **Movie 1A and 1B:** Nuclear dynamics was observed in diploid wild-type (1A, strain DHY6) and *spc72*Δ cells (1B, strain DHY19). One of the four genes coding for histone H4 was engineered to express a carboxy-terminal GFP-fusion (Wach *et al.*, 1997). Nuclear dynamics was followed for more than 9 h. Acquisition interval, 3 min; movie speed, 10 frames/s = 30 min/s. One *z*-axis plane fluorescence image was acquired.

Table 2: Dependency of nuclear migration success on nuclear positioning prior to anaphase B in wild-type and *spc72Δ* cells

Position of nucleus prior to anaphase B:						
wild-type	100%		-		-	
spc72Δ:	24.6%		63.0%		12.4%	
Nuclear migration:	successful	failed	successful	failed	successful	failed
wild-type:	100%	-	-	-	-	-
spc72Δ:	85.1%	14.9%	82.6%	17.4%	74.0%	26.0%

The relation between nuclear positioning and subsequent nuclear migration success was analyzed by time-lapse fluorescence microscopy of diploid Hhf2-GFP labeled cells. In all cases the last time-point prior to nuclear elongation was taken into account for the depicted nuclear positioning. Nuclear migration was counted as failed when the nucleus had not entered the bud at the time the cell started a new cell cycle with new bud emergence. Later entry of a nucleus into a bud from a previous cell cycle was not observed. (wild-type n=120, *spc72Δ* n=219).

Orientation of the elongating nucleus and presumably the spindle along the mother-bud axis, which is typical for wild-type cells, frequently did not occur in the *spc72*Δ mutant. In 53% of all mutant cells nuclear elongation was not oriented along the mother-daughter axis (Table 3). Early insertion of the anaphase nucleus into the bud neck was never observed in *spc72*Δ cells, whereas this was always the case for wild-type cells (Movie 1A). Hence, elongation of the anaphase nucleus occurred in mother cells of the *spc72*Δ mutant. Also, rapid oscillations and occasional bending of the elongated nucleus commonly observed for anaphase in wild-type cells were completely absent in the mutant.

Spindle Positioning and Orientation Defects Can Be Rescued in spc72Δ Cells

In *S. cerevisiae* proper nuclear segregation depends on correct nuclear positioning and on the preanaphase orientation of the mitotic spindle along the mother-daughter polarity axis. Cells displaying wrongly positioned and misoriented

Table 3: Dependency of nuclear migration success on spindle orientation in wild-type and *spc72Δ* cells

Alignment of spindle in anaphase B:	in mother-bud axis		not in mother-bud axis	
wild-type:	100%		-	
spc72Δ:	47.2%		52.8	
Nuclear migration:	successful	failed	successful	failed
wild-type:	100%	-	-	-
spc72Δ:	85.4%	14.6%	78.5%	21.5%

The relation between spindle orientation and subsequent nuclear migration success was analyzed by time-lapse fluorescent microscopy of diploid Hhf2-GFP labeled cells. Spindle orientation was counted as aligned along the mother-bud axis when the elongated nucleus pointed into the bud neck. Nuclear migration was counted as failed when the nucleus had not entered the bud at the time the cell started a new cell cycle with new bud emergence. Later entry of a nucleus into a bud from a previous cell cycle was not observed (wild-type n=120, *spc72Δ* n=203). Note that in wild-type cells the nucleus is inserted into the bud-neck early in the cell cycle (indicated by a dotted nucleus). This was never observed in *spc72*Δ cells.

spindles due to mutations often fail to correctly segregate daughter nuclei (Hoepfner *et al.*, 2000; Segal *et al.*, 2000). The observed nuclear mispositioning or spindle misorientation in *spc72*Δ cells did not severely impair the distribution of nuclei between mother and daughter cells in later cell cycle phases. As evident from Figure 1 and Movie 1B separation of both nuclear masses occurred entirely in the mother cells, frequently followed by migration of one daughter nucleus into the bud. Table 2 summarizes the consequences of correct or impaired nuclear positioning on nuclear segregation in >200 cells. Remarkably, 74% of cells with completely mispositioned nuclei still displayed successful nuclear segregation compared with 85% of cells with nuclei positioned at the bud neck. Table 3 summarizes a similar analysis of the consequences of misaligned spindles on nuclear segregation. Many cells (78%) with misaligned preanaphase spindle were able to segregate one nucleus into the bud compared with 85% of cells with a spindle oriented along the mother-bud axis.

This behavior of *spc72*Δ cells strikingly contrasts observations of *cnm67*Δ cells analyzed by the same method in the same strain background (Hoepfner *et al.*, 2000). In the SPB mutant *cnm67*Δ impaired astral microtubule organization led to the formation of bi- and multinucleate cells within a few cell cycles. In this mutant nuclear positioning and spindle orientation defects occurred significantly less frequently than in *spc72*Δ cells (27% wrongly positioned nuclei and 25% misoriented spindles in *cnm67*Δ cells) but nuclear segregation more often failed when the preanaphase nucleus was not positioned at the neck. Remarkably, the overall ratio of single to multinucleate cells was the same in both mutants when still images with large numbers of fixed log phase cells were analyzed (*spc72*Δ 34%; *cnm67*Δ 33% bi- and multinucleate cells; n = 800). Only by using time-lapse microscopy was it possible to identify characteristic differences between the viable SPB mutants *spc72*Δ and *cnm67*Δ.

Our analyses of Hhf2-GFP–expressing cells revealed that regulated nuclear positioning was basically absent and spindle orientation was drastically impaired in *spc72*Δ mutants. Nevertheless, unlike in the *cnm67*Δ mutant, many *spc72*Δ cells were able to compensate for failures in early nuclear migration steps in later cell cycle stages, the mechanism of which will be investigated below.

*Long Astral Microtubules Are Absent throughout Cell Cycle in spc72*Δ *Cells*

Nuclear migration is achieved by forces acting on the nucleus via astral microtubules (Huffaker *et al.*, 1988; Sullivan and Huffaker, 1992; Carminati and Stearns, 1997; Shaw *et al.*, 1997). Because *spc72*Δ cells frequently showed successful, although delayed, nuclear migrations it was important to investigate astral microtubule organization and dynamics in *spc72*Δ cells. Using a GFP-Tub1 fusion (Straight *et al.*, 1997), we constructed diploid wild-type and *spc72*Δ cells with fluorescently labeled microtubules. We investigated microtubule morphology over several cell cycles by time-lapse studies in a total of 76 wild-type cells (Movie 2A) and 84 *spc72*Δ cells (Movie 2B) and by acquisition of still images (Figure 2, A and B). Analysis of these data revealed a complete lack of long astral microtubules in the deletion mutant. This explains the observed impairment of early nuclear migration steps described above (Figure 1 and Table 2). Reduced astral microtubule arrays had already been described in previous studies by using *spc72-ts* and deletion mutants (Chen *et al.*, 1998; Knop and Schiebel, 1998; Souès and Adams, 1998). Our in vivo observations supported this reported lack of long astral microtubules throughout the cell cycle. We were not able to detect residual long astral microtubules early in the cell cycle mentioned in one study (Souès and Adams, 1998).

*Active Spindle Reorientation Occurs via Very Short Astral Microtubules in spc72*Δ *Cells*

Investigations of time-lapse sequences of cells with randomly oriented spindles revealed frequent reorientation of spindles despite the absence of detectable long astral microtubules (Movie 2B). This reorientation started as soon as both spindle pole bodies of the elongating spindle were close to the cell cortex. Two models could explain such a behavior: first, passive alignment of the elongating spindle along the longest cell axis of an ellipsoid-shaped cell, or second, active reorientation mediated by forces acting on the spindle. The first possibility is very unlikely, because we observed spindle reorientation events followed by successful nuclear migration independently of the ellipsoid shape of the mother cell and of the position of the bud (Figure 1, cell B, 261–321 min). An active spindle reorientation capacity of *spc72*Δ cells was apparent in time-lapse studies of haploid, more spherical cells. These studies revealed directed reorientation events of >50° within 4.5 min (Figure 3 and Movie 3). During this time the spindle elongated <0.6 μm, finally ruling out a passive random spindle movement or alignment along the longest cell axis.

To investigate the factors involved in active spindle reorientation, we performed additional time-lapse studies with higher time resolution of 15 s and higher magnification, concentrating on the phase where directed spindle reorientation was observed (Movie 4, A and B, and representative frames shown in Figure 4). Visual inspection of these movie sequences revealed very short and unstable astral microtubules emanating from the mutant SPBs that had neither been detectable in previous time-lapse studies nor still images. These observed astral microtubules never reached lengths >1 μm (n = 28) and could often be identified in a single movie frame only. In four similar cases we could follow minor growth steps of individual astral microtubules for up to four movie frames, representing 1-min real time. In the fifth frame, the microtubules were no longer detectable, suggesting that disassembly was a very rapid process. Estimations based on the measured length and observed dynamics of these microtubules suggest slower growth, faster shrinkage, and higher catastrophy frequency in *spc72*Δ cells with respect to published astral microtubules dynamics found in wild-type cells (Carminati and Stearns, 1997). In addition, in 30% of the cells analyzed by high-resolution time-lapse imaging (n = 18) it was not possible to detect short astral microtubules. In these cells, the spindle did not reorient along the mother-bud axis and nuclear segregation failed. This strongly supported the view that the observed reorientation of anaphase spindles depended on the presence of residual short astral microtubules.

A very rare event that was only observed in one of 84 cells confirmed the proposed capability of *spc72*Δ cells to form residual microtubules in the absence of the Spc72 protein. In this cell (Movie 5, and representative frames in Figure 5)

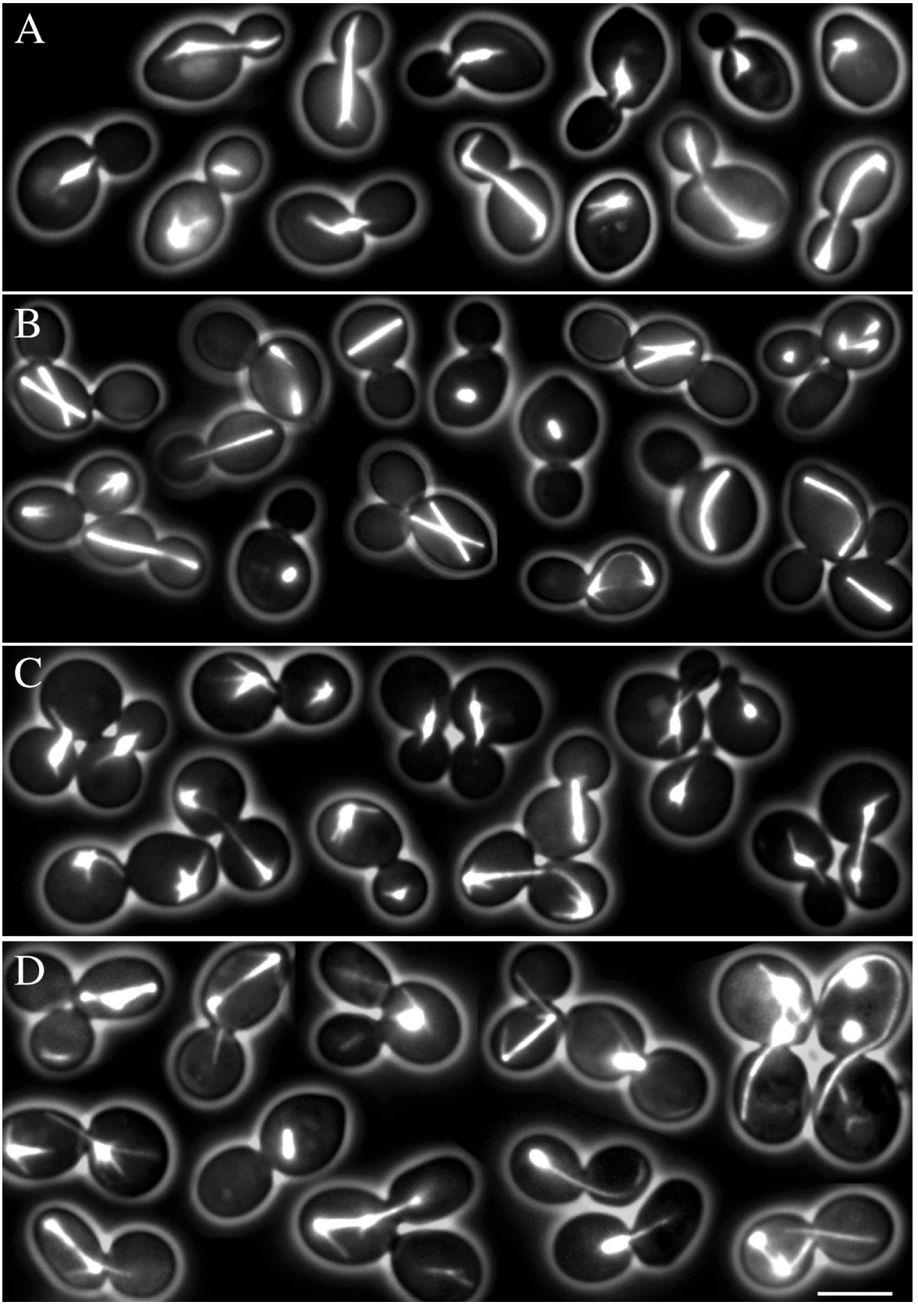
A
B
C
D

astral microtubules generated at one SPB grew much longer than observed in all other *spc72*Δ cells. These long astral microtubules detached after having contacted the cell cortex and were pulled into the bud. Unlike in *cnm67*Δ cells where detached astral microtubules (carrying Spc72p at one end) were stable for >30 min (Hoepfner *et al.*, 2000), detached astral microtubules in the *spc72*Δ cell were rapidly degraded within a few minutes.

Our observations suggest that spindle poles lacking the Spc72 protein are able to nucleate only unstable astral microtubules which, with rare exception, are very short. These residual short astral microtubules are essential to reorient misoriented spindles upon cortex contact; however, they are not capable of positioning G1-phase nuclei in *spc72*Δ cells because longer astral microtubules that span the SPB-cortex distance would be required to perform this task.

*spc72*Δ *Is Synthetically Lethal with Loss of Kar3 or Cnm67*

It is conceivable that directed force production via residual astral microtubules is responsible for the observed spindle reorientation in *spc72*Δ cells. Such mechanism would require the action of motor proteins (reviewed by Hildebrandt and Hoyt, 2000) and possibly cortical determinants (Farkasovsky and Küntzel, 1995; Miller and Rose, 1998; Yeh *et al.*, 2000). To genetically test this hypothesis, we constructed a set of *spc72*Δ double mutants carrying deletions for known astral microtubule motor genes and genes of cortical determinants such as *KIP2*, *KIP3*, *KAR3*, *DHC1*, *KAR9*, and *NUM1* (Meluh and Rose, 1990; Eshel *et al.*, 1993; Li *et al.*, 1993; Farkasovsky and Küntzel, 1995; Carminati and Stearns, 1997; Cottingham and Hoyt, 1997; DeZwaan *et al.*, 1997; Saunders *et al.*, 1997; Miller and Rose, 1998; Yeh *et al.*, 2000). Six different heterozygous diploids each carrying two deletions were constructed by mating of the respective haploids. Afterward, they were subjected to tetrad analysis, including verification

Figure 2 (facing page). Microtubule morphologies at different cell cycle stages in *S. cerevisiae* wild-type cells and in two spc72 mutants. Representative cells with GFP-labeled microtubules were selected from still pictures. (A) Wild type. In unbudded cells an array of astral microtubules is visible, eventually interacting with the cortex. In small budded cells the spindle poles separate and a short thick spindle is formed. Astral microtubules interact with the bud, position the nucleus, and orient the spindle. In large budded cells astral microtubules interacting with the cortex are prominent. (B) *Spc72*Δ mutant. Long astral microtubules are completely absent throughout the cell cycle. As in wild-type cells, spindles are clearly visible as short or long bars, but are frequently misoriented. Misoriented long spindles appear bent. Multibudded cells contain more than one spindle. Short microtubules similarly oriented as the spindle are most likely nuclear microtubules. (C) *Spc72*Δ *spc72-7* cells grown at 23°C. Microtubule numbers, morphologies, and orientations are indistinguishable from wild type. (D) *Spc72*Δ *spc72-7* cells grown at 37°C. Astral microtubules are clearly visible and appear significantly longer than in wild-type cells. Only very few cells show reduced or no astral microtubules. In many cells astral microtubules are detached from the SPB region. Some of the detached microtubules are extremely long. Cells with multiple and misaligned spindles are present. Cells with more than one spindle possess more than one bud. All cell images of this figure represent merged still images of five *z*-axis planes. Bar, 5 μm. **Movie 2A.** Microtubule dynamics in wild-type cells (strain DHY209) expressing GFP-Tub1 followed for 2.5 h. Acquisition interval, 2 min; movie speed, 10 frames/s = 20 min/s. Three *z*-axis plane fluorescence images were acquired and merged. **Movie 2B.** Microtubule dynamics in *spc72*Δ cells (strain DHY208) expressing GFP-Tub1 followed for 8 h. Acquisition interval, 2 min; movie speed, 10 frames/s = 20 min/s. Three *z*-axis plane fluorescence images were acquired and merged.

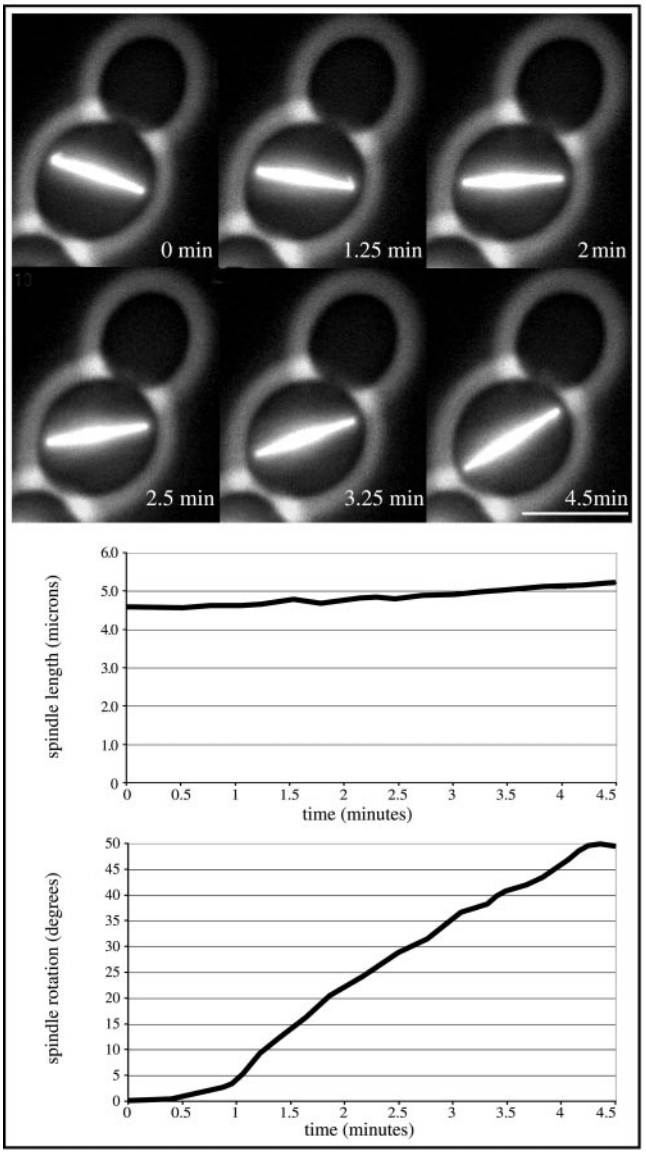

Figure 3. Kinetics of spindle reorientation process in a spc72Δ cell (strain DHY205). Top, representative frames of Movie 3. Within 4.5 min the misoriented spindle rotates >50°C. Short astral microtubules, possibly mediating this rotation, are visible at 0 min at the left SPB and at 1.25 min at the right SPB. Bar, 5 μm. Middle, length of the rotating spindle plotted against the rotation time. Bottom, rotation angle of the spindle plotted against the rotation time. **Movie 3.** Time-lapse sequence of the spindle reorientation process analyzed in Figure 3. Acquisition interval, 15 s; movie speed, 10 frames/s = 3 min/s. Three *z*-axis plane fluorescence images were acquired and merged.

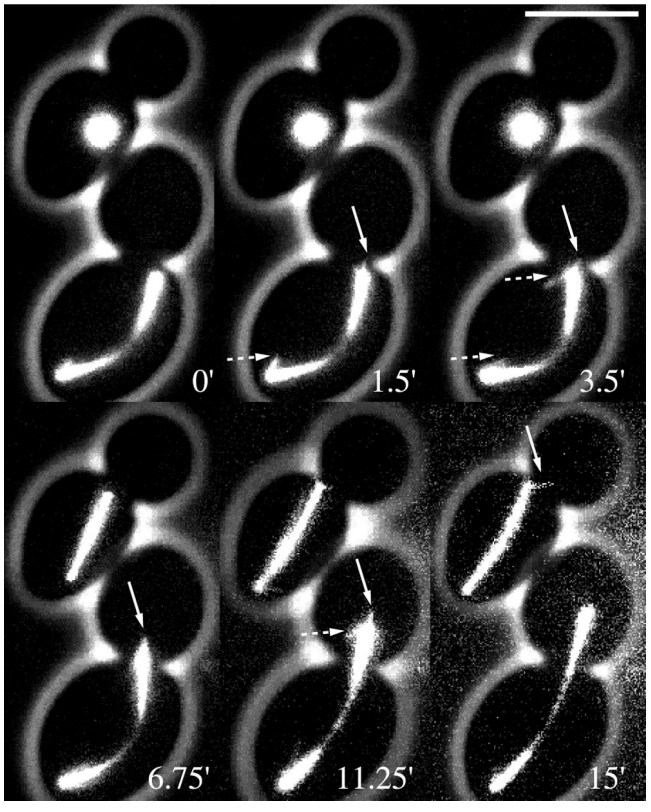

Figure 4. Residual short and unstable astral microtubules in *spc72*Δ cells. Six images of the high-resolution time-lapse sequence of Movie 4A are shown. In the lower cell the already elongated spindle is misoriented and mislocalized (0′). Short astral microtubules are visible during the reorientation of the spindle. Further spindle elongation leads to penetration of the spindle through the bud neck (3.5′–15′). The upper cell enters anaphase without properly localizing the spindle to the bud neck. Although the orientation of the spindle almost points into the bud, penetration is not observed before the spindle spans the whole length of the cell. At 15′ one short astral microtubule is seen at the upper SPB pointing into the bud. Microtubules indicated with solid arrows are astral microtubules evidenced by the orientation angle relative to the spindle. Microtubules indicated with dotted arrows are either nuclear microtubules or astral microtubules with orientation angles relative to the spindle not observed in wild-type cells. Bar, 5 μm. **Movie 4, A and B.** Short astral microtubules and spindle reorientation in GFP-Tub1 expressing *spc72*Δ (strain DHY208) cells followed for 15 and 20 min, respectively. Acquisition interval, 15 s; movie speed, 10 frames/s = 2.5 min/s. Three z-axis plane fluorescence images were acquired and merged.

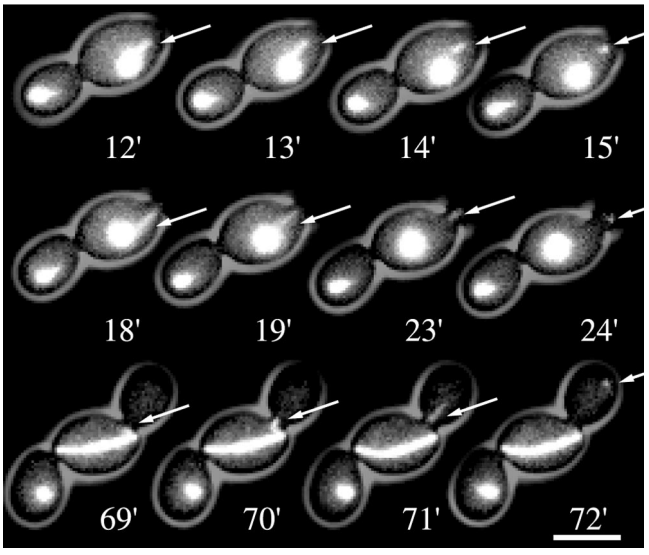

Figure 5. Astral microtubule formation and detachment observed in one *spc72*Δ cell. Representative frames of Movie 5 are shown. At bud emergence one astral microtubule longer than 1 μm, interacting with the site of the nascent bud, can be seen (0′). Unlike in wild-type cells this does not result in movement of the nucleus toward the bud neck; instead, the astral microtubule detaches from the SPB region and is pulled into the small bud (13′–15′). A new astral microtubule is formed that also detaches after interaction with the bud cortex and moves into the bud (18′–24′). After spindle elongation new astral microtubules are formed that presumably try to reorient the misaligned spindle. These astral microtubules also detach (69′–72′). As apparent in the corresponding time-lapse movie no more long astral microtubule formation can be observed at later time points. The cell shows failed nuclear migration and follows all mutant characteristics observed in other *spc72*Δ cells. Bar, 5 μm. **Movie 5.** Time-lapse study of growth and detachment of astral microtubules in a *spc72*Δ cell (strain DHY208) followed for 3 h. Cells express an amino-terminal GFP-Tub1 fusion (Straight *et al*., 1997). Acquisition interval, 1min; movie speed, 10 frames/s = 10 min/s. Three *z*-axis plane fluorescence images were acquired and merged.

of the deletion alleles in the growing colonies by PCR and by identification of the deletion-associated markers (Figure 6). We obtained four viable colonies from all tested heterozygous diploids except for *spc72*Δ*/SPC72 kar3*Δ*/KAR3* (Figure 6). Microscopy of the nonviable *spc72*Δ*/kar3*Δ spores revealed that they germinated but then arrested as large, multibudded cells (our unpublished data). The other double mutants grew as slowly as the *spc72*Δ single mutants.

We also genetically tested the hypothesis that active spindle reorientation and thus viability depended on residual astral microtubules in *spc72*Δ cells. If so, further impairing the remaining astral microtubule formation at the SPB outer plaque in *spc72*Δ cells by deletion of *CNM67* should be lethal. Loss of Cnm67 has been shown to result in the loss of the SPB outer plaque, which exclusively impaired the formation of astral microtubules at this substructure, without altering the dynamics of spindle microtubules nor the formation of astral microtubules at the half-bridge (Brachat *et al*., 1998; Hoepfner *et al*., 2000). Tetrad analysis of the heterozygous diploid *spc72*Δ*/SPC72 cnm67*Δ*/CNM67* revealed that the *spc72*Δ*/cnm67*Δ double mutant was nonviable (Figure 6, bottom). Microscopy of the *spc72*Δ*/cnm67*Δ spores showed that they germinated and then arrested as multibudded cells. In summary, in a *spc72*Δ background, single deletion of four astral microtubule motors, two astral microtubule–cortex interaction mediators, and one other SPB outer plaque component revealed synthetic lethality of *spc72*Δ only in the absence of the microtubule motor Kar3 and the SPB component Cnm67, respectively. This allows the conclusion that short astral microtubules organized by the SPB outer plaque in the *spc72*Δ mutant are essential for reorientation of misaligned spindles.

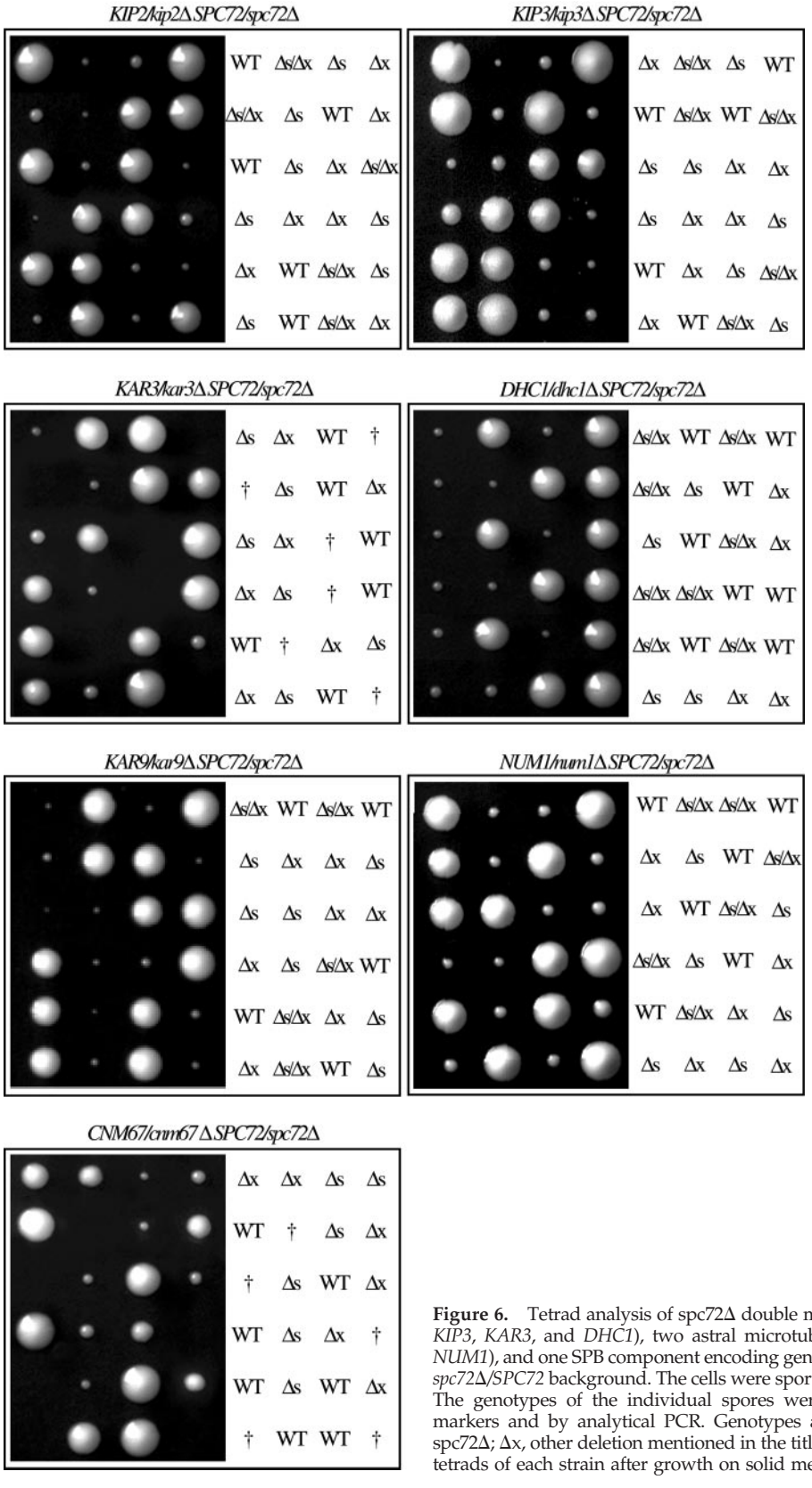

Figure 6. Tetrad analysis of spc72Δ double mutants. Four astral microtubule motors (*KIP2*, *KIP3*, *KAR3*, and *DHC1*), two astral microtubule–cortex interaction mediators (*KAR9* and *NUM1*), and one SPB component encoding genes have been deleted in a heterozygous diploid *spc72*Δ/*SPC72* background. The cells were sporulated and the asci subjected to tetrad analysis. The genotypes of the individual spores were determined by the segregation of genetic markers and by analytical PCR. Genotypes are indicated as follows: WT, wild type; Δs, spc72Δ; Δx, other deletion mentioned in the title; †, lethal. The figure shows six representative tetrads of each strain after growth on solid medium for 4 d.

Table 4. Spindle dynamics in wild-type and mutant cells

Strain	Unelongated spindle length	Breakdown length	Anaphase duration	Fast elongation	Slow elongation	n
	μm	μm	min	μm/min	μm/min	
Wild-type 2n	1.98	13.25	28.2	0.78	0.23	30
	$\sigma = 0.08$	$\sigma = 0.42$	$\sigma = 3.1$	$\sigma = 0.06$	$\sigma = 0.03$	
Δ*spc72*/Δ*spc72* 2n	2.01	12.81	32.1	0.78	0.24	25
	$\sigma = 0.12$	$\sigma = 0.51$	$\sigma = 4.2$	$\sigma = 0.06$	$\sigma = 0.03$	
Wild-type 1n[a]	2.02	10.50	21.8	0.73	0.26	20
	$\sigma = 0.11$	$\sigma = 0.49$	$\sigma = 2.8$	$\sigma = 0.07$	$\sigma = 0.02$	
Δ*kar3* 1n[b]	1.98	10.90	22.6	0.81	0.24	15
	$\sigma = 0.14$	$\sigma = 0.72$	$\sigma = 2.4$	$\sigma = 0.08$	$\sigma = 0.09$	

[a] In haploid wild-type cells anaphase B was observed 62 min ($\sigma = 12$) after bud emergence.

[b] In Δ*kar3* cells anaphase B was observed 98 min ($\sigma = 22$ min) after bud emergence.

To investigate in more detail the terminal phenotype of *kar3*Δ *spc72*Δ and *cnm67*Δ *spc72*Δ cells, we used the ts allele spc72-7 (Knop and Schiebel, 1998) to construct conditional *cnm67*Δ *spc72*Δ *spc72-7* and *kar3*Δ *spc72*Δ *spc72-7* mutants. Unfortunately, when shifted 37°C, we were not able to induce synthetic lethality. However, we found an interesting phenotype and astral microtubule morphology in control *spc72*Δ cells carrying the *spc72-7* allele and the *GFP-TUB1* fusion gene. At 23°C the *spc72-7* allele complemented the *spc72*Δ phenotype; long astral microtubules emanated from the spindle poles and elongating spindles were correctly oriented (Figure 2C). After 5-h incubation at 37°C cells did not stop dividing. Long astral microtubules still emanated from the spindle poles, however, many cells contained detached long and apparently stable microtubules (Figure 2D). In addition, a substantial fraction of the spindles were misoriented, probably due to an unstable anchoring of astral microtubules at the half-bridge or outer spindle pole plaque. The detached microtubules in these cells may still be associated with the Spc72 mutant protein because microtubules detaching from the spindle pole together with the Spc72 anchor are very stable (Hoepfner *et al.*, 2000)

Spindle Elongation Dynamics Is Unaffected by Loss of Spc72 or Kar3

As evidenced in our time-lapse sequences, final transit of a nucleus through the bud neck in *spc72*Δ cells, after successful reorientation via short astral microtubules, was dependent on the final elongation phase of the spindle. The first phase of spindle elongation, including separation of the nuclear masses was always restricted to the mother cell. When the spindle was as long as the diameter of the mother cell and when it continued to elongate we did observe transit of one SPB through the bud neck (n = 203). Transit of a nucleus through the bud neck after spindle breakdown in the mother cell was never observed.

Because spindle dynamics significantly contributed to nuclear migration success, it was important to verify that the observed synthetic lethality of *spc72*Δ *cnm67*Δ and *spc72*Δ *kar3*Δ double mutants was caused by astral microtubule-related functions and not by altered spindle elongation kinetics. In previous time-lapse experiments it was already shown that loss of the cytoplasmic SPB component Cnm67 did not alter spindle kinetics compared with wild-type cells (Hoepfner *et al.*, 2000). However, genetic screens and functional analyses implicated Kar3 in spindle functions (Meluh and Rose, 1990; Page and Snyder, 1992; Cottingham *et al.*, 1999; Manning *et al.*, 1999) and loss of Spc72 was also suggested to interfere with spindle dynamics (Chen *et al.*, 1998; Knop and Schiebel, 1998). Using a GFP-Tub1 label (Straight *et al.*, 1997) and time-lapse microscopy at 1-min intervals, we measured parameters of spindle kinetics in wild-type, *spc72*Δ, and *kar3*Δ cells (Table 4). Our results of wild-type cells were very similar to published data obtained using the same GFP label (Straight *et al.*, 1998). All five parameters measured in *spc72*Δ cells were similar to wild type, strongly suggesting no involvement of the Spc72 protein in nuclear microtubule functions.

Similarly, *kar3*Δ cells showed spindle elongation and spindle breakdown kinetics comparable to wild type. However, onset of anaphase B was significantly delayed (Table 4). Time-lapse movies (our unpublished data) revealed impaired formation of short, bar-shaped spindles and many cells formed a diffuse array of nuclear microtubules as already observed in previous studies on Kar3 function (Meluh and Rose, 1990; Saunders *et al.*, 1997; Cottingham *et al.*, 1999). Nevertheless, all cells finally assembled a bipolar spindle and successfully executed anaphase. Thus, loss of Kar3 impairs spindle assembly, which delays onset of anaphase but does not affect the elongation kinetics per se. Because it is the spindle elongation that contributes to the viability of *spc72*Δ cells and because this process is not impaired by loss of the Kar3 motor it seems very likely that the observed synthetic lethality of *spc72*Δ *kar3*Δ cells is caused by loss of the astral microtubule-associated function of Kar3 and not by loss of its role in spindle assembly.

Consequences of Failed Nuclear Segregations

Spc72Δ cells that failed to direct one nucleus into the bud finished the cell cycle with a binucleate mother cell and an anucleate bud. These aberrant segregation events, however, did not trigger a permanent growth arrest, and the binucleate cells initiated without delay a new cell cycle as seen by new bud emergence, SPB duplication, spindle assembly, and

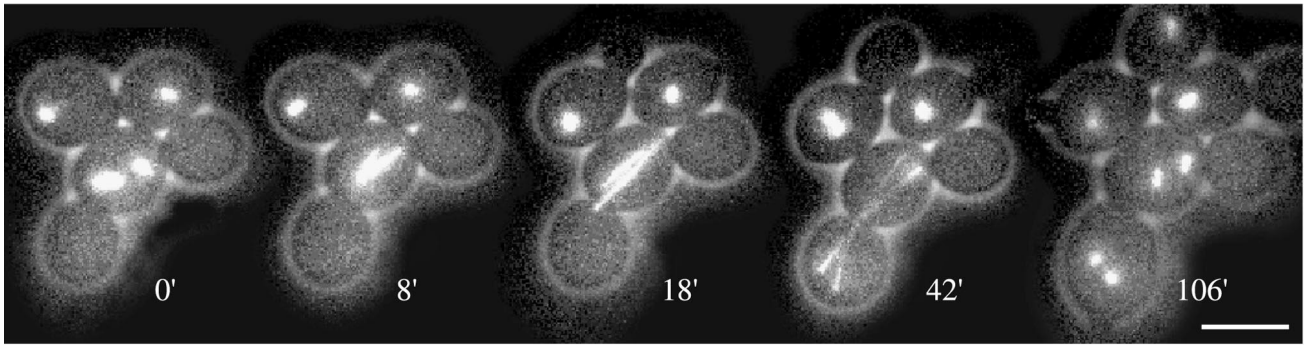

Figure 7. Simultaneous segregation of two daughter nuclei after mitosis in a binucleate *spc72*Δ cell. Representative frames of Movie 7A are shown. Two mispositioned and misoriented short spindles are visible in a mother cell with two buds; the emerging bud of the current cell cycle is the lower one (0′). Both spindles enter anaphase B simultaneously (8′). Reorientation of both spindles results in subsequent insertion of both spindles into the bud (18′–42′). After spindle breakdown and cytokinesis bud emergence is visible in the newborn binucleate daughter cell (106′). Bar, 5 μm. Similar translocation of two nuclei into one bud was also observed in spc720 cells with histone-GFP labeled nuclei, in Movie 7B. **Movie 7A.** Translocation of two daughter nuclei during one cell cycle of a binucleate *spc72*Δ cell. Proliferation of GFP-Tub1 expressing *spc72*Δ cells (strain DHY209) was followed for 5 h. Acquisition interval, 2 min; movie speed, 10 frames/s = 20 min/s. Three *z*-axis plane fluorescence images were acquired and merged. **Movie 7B.** Translocation of two daughter nuclei during one cell cycle of a binucleate *spc72*Δ cell. Proliferation of Hhf2-GFP expressing *spc72*Δ cells (strain DHY19) was followed for 6.5 h. Acquisition interval, 1 min; movie speed, 10 frames/s = 10 min/s. One *z*-axis plane fluorescence image was acquired.

simultaneous mitotic divisions of the two nuclei (Figure 1, cell A, 141–324 min, and Movie 2B). Further nuclear segregation failures in the pedigrees of binucleate cells led to multinucleate cells. A frequent generation of binucleate mother cells with attached anucleate bud, followed by nuclear segregation failures during new cell cycles, was already observed for cnm67Δ the outer plaque deletion mutant (Hoepfner *et al.*, 2000). A log phase culture of spc72Δ cells showed the following distribution: 69.5% with one nucleus, 18.5% with two nuclei, 3.2% with three nuclei, 7% with four nuclei, and 8% with five or more nuclei (n = 800). The frequency of cells with even numbers of nuclei was slightly higher compared with cnm67Δ cells, although cnm67Δ cells showed the same ratio of single-to-multinucleate cells. This could be explained by the observation that multinucleate spc72Δ cells sometimes transferred more than one nucleus into a nascent bud (Figure 7 and Movie 7, A and B), leading to an initially binucleate daughter cell. Such an event was never observed in cnm67Δ cells (n = 325; Hoepfner *et al.*, 2000) but occurred in 12% of bi- or multinucleate spc72Δ cells (n = 220). As in cnm67Δ cells, deposition of a nucleus into a still attached anucleate bud of a previous cell cycle was never detected.

We were also able to monitor cell separation in wild-type and spc72Δ cells, which was evidenced by a sudden change in the position of the bud relative to that of the mother cell (Figure 1, cells A and B, 63–99 min, and Movies 1 and 2, A and B). In wild-type and spc72Δ cells, separation of nucleate buds from the mother cell occurred ~30 min after entry of the nucleus into the bud. However, anucleate buds in spc72Δ cells stayed permanently attached to their mother cells (Figure 1, cell A, 195–483 min; cell B, 372–483 min; and Movies 1B and 2B). These observations suggest a link between successful nuclear migration and cell separation in spc72Δ mutants as was already observed in cnm67Δ cells (Hoepfner *et al.*, 2000). The formation of anucleate cells that were counted in cultures of fixed cells in other studies (Chen *et al.*, 1998; Knop and Schiebel, 1998; Souès and Adams, 1998) could therefore not be recapitulated during in vivo time-lapse studies.

During our analyses it became apparent that the first nuclear migration event in newborn daughter cells was always successful despite the absence of long astral microtubules. Nuclear migrations in later cell cycles showed a constant failure ratio. Such an age-dependent characteristic has already been reported for *cnm67*Δ cells and was shown not to be related to cell size, budding pattern, or the presence of the She1 protein (Hoepfner *et al.*, 2000). This points toward a general mother-daughter difference in nuclear migration rather than an *spc72*Δ- or *cnm67*Δ-specific characteristic.

DISCUSSION

*spc72*Δ *Cells Organize Residual Short and Unstable Astral Microtubules*

We used in vivo time-lapse analysis of cells with labeled nuclei and microtubules to compare nuclear migration and microtubule behavior of wild-type and *spc72*Δ cells. We examined why the absence of Spc72 is not lethal as would be predicted by its previously proposed function as anchor for the cytoplasmic γ-tubulin complex (Knop and Schiebel, 1998; Pereira *et al.*, 1999). In this study, we could show that loss of Spc72 resulted in lack of long astral microtubules but very short and unstable astral microtubules persisted. These short astral microtubules were unable to cover long distances from the SPB to the cortex early in the cell cycle, resulting in a strong nuclear positioning and spindle orientation defect. However, upon spindle elongation and contact of the SPB with the cortex, these short astral microtubules were able to reorient the elongating spindle. As soon as the spindle had been successfully reoriented in *spc72*Δ cells, spindle elongation proceeded with wild-type kinetics, resulting in the penetration of one SPB through the bud neck. This frequently led to delayed but successful segregation of the chromosomal masses. Thus, our time-lapse sequences

showed that successful nuclear migrations were not stochastic events as suggested in other studies but depended on forces acting via the residual astral microtubules.

Revised Model for Spc72 Function

Our findings allow new interpretations of previously published results. The residual astral microtubules in this study and the integrity of the SPB outer plaque in the absence of Spc72 suggest the presence of at least one other γ-tubulin complex binding protein at the SPB outer plaque. This hypothesis is in agreement with several other published experimental results. First, in vegetatively growing wild-type cells only a small percentage of the γ-tubulin complex directly interacts with Spc72 (Knop and Schiebel, 1998). Second, only a small percentage of Spc72 interacts with Nud1, which forms the proposed interaction site at the outer plaque (Gruneberg *et al*., 2000). Third, loss of Cnm67 and Nud1 but not Spc72 causes loss of the SPB outer plaque (Brachat *et al*., 1998; Chen *et al*., 1998; Souès and Adams, 1998; Adams and Kilmartin, 1999; Gruneberg *et al*., 2000). Finally, although loss of the SPB outer plaque is observed in mutants with N-terminal truncations of the Cnm67 protein, in 25% of the cases observed by electron microscopy, astral microtubules appeared to be still organized by the cytoplasmic face of the SPB (Schaerer *et al*., 2001). Together with our observation that deletion of the central region of Cnm67 is synthetic lethal in an *spc72*Δ background, this suggests the existence of a factor that interacts with the central region of Cnm67 and is capable of organizing astral microtubules.

Several findings support the notion that Spc72 is the only γ-tubulin complex anchor at the half-bridge. First, in the absence of Spc72 loss of the SPB outer plaque results in a lethal phenotype, indicating that the observed residual microtubules in *spc72*Δ cells are not organized by the half-bridge structure. Second, in the absence of the SPB outer plaque lethality is still observed in the presence of Spc72 if the first 15 amino acids of Kar1, which comprises the Spc72 interaction site at the half-bridge, are missing (Pereira *et al*., 1999). Thus, impairing the known Spc72 anchor site at the half-bridge apparently abolishes astral microtubule formation from this SPB substructure.

As shown recently, the formation of astral microtubules by two different SPB substructures seems to be controlled via phosphorylation of Spc72: Nud1 preferentially interacts with phosphorylated Spc72 that starts to appear at G2/S transition (Gruneberg *et al*., 2000). This is in agreement with our previous observation that astral microtubules and the Spc72 protein switch from the half-bridge to the outer plaque as visualized by time-lapse microscopy (Hoepfner *et al*., 2000). In the context of this study, the following model is in better agreement with the experimental data: in the early stages of the cell cycle Spc72 is the astral microtubule anchor at the half-bridge. On G2/S transition Spc72 is phosphorylated and astral microtubules are switched to the outer plaque where they are maintained by a second γ-tubulin anchor.

Finally, we suggest that the observed astral microtubule instability in *spc72*Δ cells is due to impaired organization of Stu2, an essential protein, that was shown to laterally bind microtubules and interact with Spc72 (Wang and Huffaker; 1997; Chen *et al*., 1998). It was speculated that the lateral binding capability of Stu2 could maintain the attachment of microtubules to the pole, even during subunit exchange at the ends (Wang and Huffaker, 1997). Involvement of Stu2 in microtubule anchoring is now supported by the observed microtubule detachment upon shift to the nonpermissive temperature in Spc72-ts cells. Astral microtubule detachment was also observed in the very rare cases where astral microtubules longer than 1 μm were formed in *spc72*Δ deletion mutants. These astral microtubules were very unstable and were rapidly degraded. In the previously analyzed *cnm67*Δ SPB mutant, detached astral microtubules appeared to be much more stable, most likely because these microtubules were still capped with the γ-tubulin complex (Hoepfner *et al*., 2000). Therefore, we conclude that in the absence of Spc72, Stu2-dependent microtubule anchoring to the γ-tubulin complex is impaired and microtubule stability reduced. Microtubules that are able to achieve detectable lengths detach from the γ-tubulin complex and thus the SPB and are rapidly degraded. During the reviewing process of this article, new evidence was published supporting our model. Detailed analyses of conditional Stu2 mutants revealed that Stu2 plays a prominent role in determining assembly properties of astral microtubules (Kosco *et al*., 2001).

Spindle Reorientation Is Dependent on Kar3 but Not Kar9/Myo2 Pathway

Our analysis of double mutants with *spc72*Δ revealed synthetic lethality with the microtubule motor Kar3. Based on our data, we believe that this is not due to the involvement of Kar3 in spindle assembly, but due to its function on astral microtubules. Loss of Kar3 was shown to increase the length of astral microtubules (Saunders *et al*., 1997). Longer astral microtubules would facilitate spindle orientation in *spc72*Δ cells. Because this was not the case, we believe that it is the actual motor function of Kar3 that is involved in the observed spindle reorientation in *spc72*Δ cells. To our surprise, no synthetic effect was observed in *spc72*Δ *kip3*Δ cells although several experiments suggest redundant functions of Kip3 and Kar3 in nuclear positioning and spindle orientation (Miller *et al*., 1998; Cottingham *et al*., 1999). Furthermore, loss of Kar9 did not additionally impair growth of *spc72*Δ cells despite recent findings that Kar9 is involved in a capturing process of Bim1-coated microtubules, which are then directed along actin cables into the bud by translocation of Myo2, a class V myosin (Beach *et al*., 2000; Miller *et al*., 2000; Yeh *et al*., 2000; Yin *et al*., 2000). Apparently, in the absence of Kar3, neither Kip3 nor Kar9, in conjunction with Myo2, is sufficient to perform the observed reorientation of spindles in *spc72*Δ cells observed in this study.

It therefore appears that Kar3 is the most efficient motor producing force on the nucleus during astral microtubule-mother cell cortex interactions. This is also reflected by the observation that cells expressing Kar3 as the only astral microtubule motor are viable (Cottingham *et al*., 1999). In addition, a previous study focusing on the spindle pole *cnm67*Δ mutant showed that deletion of Kar3 caused a much more severe nuclear migration impairment than deletion of any other astral microtubule motor or Kar9 (Hoepfner *et al*., 2000).

*spc72*Δ *Cells Show Mother-Daughter Differences in Nuclear Segregation Fidelity Like cnm67*Δ *Cells*

Long-term time-lapse investigations allowed pedigree analysis of *spc72*Δ cells. This revealed that the first mitosis of newborn, single-nucleate daughter cells was always successful despite absence of long astral microtubules. Later divisions of the same cells often failed. We observed the same phenomenon in *cnm67*Δ SPB mutants (Hoepfner *et al.*, 2000). These observations suggest a general mother-daughter difference in nuclear migration rather than an *spc72*Δ-specific characteristic. Successful first division of daughter cells persisted independently of the cell size, budding pattern or the presence of the She1 protein (Hoepfner *et al.*, 2000), suggesting a possible change in the spindle pole structure itself is affecting the mode of nuclear migration. Maturation of centrioles has been described in mammalian cells where newly assembled centrioles were shown to be unable to perform the functions of centrioles generated in the previous cell cycle (Piel *et al.*, 2000). However, the complete lack of early spindle orientation control in *spc72*Δ cells as apparent in the time-lapse sequences rather suggests that *spc72*Δ cells have lost control over which SPB finally enters the bud. Therefore, although SPB maturation describes an exciting explanation for the mother-daughter specific differences in nuclear migration it cannot explain the behavior of the *spc72*Δ mutant because sometimes also the "old" SPB might be inserted into the bud.

ACKNOWLEDGMENTS

We thank E. Schiebel for the p*spc72-7* plasmid and A.F. Straight for the pAFS125 plasmid. We are grateful to Robbie Loewith and Amy Gladfelter for careful reading of the manuscript. This work was supported by grants from the Swiss Federal Office for Education and Science (grant 95.0191-12) and the Swiss National Science Foundation (grant 31-55941.98).

REFERENCES

Adams, I.R., and Kilmartin, J.V. (1999). Localization of core spindle pole body (SPB) components during SPB duplication in *Saccharomyces cerevisiae*. J. Cell Biol. *4*, 809–823.

Beach, D.L., Thibodeaux, J., Maddox, P., Yeh, E., and Bloom, K. (2000). The role of the proteins Kar9 and Myo2 in orienting the mitotic spindle of budding yeast. Curr. Biol. *10*, 1497–1506.

Bullock, W.O., Fernandez, J.M., and Short, J.M. (1987). XLl-Blue: a high efficiency plasmid transforming recA *Escherichia coli* strain with β-galactosidase selection. BioTechniques *5*, 376–378.

Brachat, A., Kilmartin, J.V., Wach, A., and Philippsen, P. (1998). *Saccharomyces cerevisiae* cells with defective spindle pole body outer plaques accomplish nuclear migration via half-bridge-organized microtubules. Mol. Biol. Cell *9*, 977–991.

Byers, B., and Goetsch, L. (1975). Behavior of spindles and spindle plaques in the cell cycle and conjugation of *Saccharomyces cerevisiae*. J. Bacteriol. *124*, 511–523.

Carminati, J.L., and Stearns, T. (1997). Microtubules orient the mitotic spindle through dynein-dependent interactions with the cell cortex. J. Cell Biol. *138*, 629–641.

Chen, X.P., Yin, H., and Huffaker, T.C. (1998). The yeast spindle pole body component Spc72p interacts with Stu2p and is required for proper microtubule assembly. J. Cell Biol. *141*, 1169–1179.

Cottingham, F.R., Gheber, L., Miller, D.L., and Hoyt, M.A. (1999). Novel roles for *Saccharomyces cerevisiae* mitotic spindle motors. J. Cell Biol. *147*, 335–350.

Cottingham, F.R., and Hoyt, M.A. (1997). Mitotic spindle positioning in *Saccharomyces cerevisiae* is accomplished by antagonistically acting microtubule motor proteins. J. Cell Biol. *138*, 1041–1053.

DeZwaan, T.M., Ellingson, E., Pellman, D., and Roof, D.M. (1997). Kinesin-related *KIP3* of *Saccharomyces cerevisiae* is required for a distinct step in nuclear migration. J. Cell Biol. *138*, 1023–1040.

Eshel, D., Urrestarazu, L.A., Vissers, S., Jauniaux, J.C., van Vliet-Reedijk, J.C., Planta, R.J., and Gibbons, I.R. (1993). Cytoplasmic dynein is required for normal nuclear segregation in yeast. Proc. Natl. Acad. Sci. USA *90*, 11172–11186.

Farkasovsky, M., and Küntzel, H. (1995). Yeast Num1p associates with the mother cell cortex during S/G2 phase and affects microtubular functions. J. Cell Biol. *131*, 1003–1014.

Geissler, S., Pereira, G., Spang, A., Knop, M., Souès, S., Kilmartin, J., and Schiebel, E. (1996). The spindle pole body component Spc98p interacts with the γ-tubulin-like Tub4p of *Saccharomyces cerevisiae* at the sites of microtubule attachment. EMBO J. *15*, 3899–3911.

Guthrie, C., and Fink, G.R. (1991). Guide to yeast genetics and molecular biology. Methods Enzymol. *194*, 14–15.

Gruneberg, U., Campell, K., Simpson, C., Grindlay, J., and Schiebel, E. (2000). Nud1 links astral microtubule organization and the control of exit from mitosis. EMBO J. *19*, 6475–6488.

Hildebrandt, E.R., and Hoyt, A.M. (2000). Mitotic motors in *Saccharomyces cerevisiae*. Biochim. Biophys. Acta *1496*, 99–116.

Hoepfner, D., Brachat, A., and Philppsen, P. (2000). Time-lapse video microscopy reveals astral microtubule detachment in the yeast spindle pole mutant. cnm67. Mol. Biol. Cell *11*, 1197–1211.

Huffaker, T.C., Thomas, J.H., and Botstein, D. (1988). Diverse effects of beta-tubulin mutations on microtubule formation and function. J. Cell Biol. *106*, 1997–2010.

Huxley, C., Green, E.D., and Dunham, I. (1990). Rapid assessment of *S. cerevisiae* mating type by PCR. Trends Genet. *6*, 236.

Hyman, A.A. (1989). Centrosome movement in the early divisions of *Caenorhabditis elegans*: a cortical site determining centrosome position. J. Cell Biol. *109*, 1185–1193.

Jacobs, C.W., Adams, A.E., Szaniszlo, P.J., and Pringle, J.R. (1988). Functions of microtubules in the *Saccharomyces cerevisiae* cell cycle. J. Cell Biol. *107*, 1409–1426.

Kilmartin, J.V., and Goh, P.Y. (1996). Spc110p: assembly properties and role in the connection of nuclear microtubules to the yeast spindle pole body. EMBO J. *15*, 4592–4602.

Knop, M., Pereira, G., Geissler, S., Grein, K., and Schiebel, E. (1997). The spindle pole body component Spc97p interacts with the gamma-tubulin of *Saccharomyces cerevisiae* and functions in microtubule organization and spindle pole body duplication. EMBO J. *16*, 1550–1564.

Knop, M., and Schiebel, E. (1997). Spc98p and Spc97p of the yeast γ-tubulin complex mediate binding to the spindle pole body via their interaction with Spc110p. EMBO J. *16*, 6985–6995.

Knop, M., and Schiebel, E. (1998). Receptors determine the cellular localization of a gamma-tubulin complex and thereby the site of microtubule formation. EMBO J. *17*, 3952–3967.

Knop, M., Siegers, K., Pereira, G., Zachariae, W., Winsor, B., Nasmyth, K., and Schiebel, E. (1999). Epitope tagging of yeast genes using a PCR-based strategy: more tags and improved practical routines. Yeast *15*, 963–972.

Kosco, K.A., Pearson, C.G., Maddox, P.S., Wang, P.J., Adams, I.R., Salmon, E.D., Bloom, K., and Huffaker, T.C. (2001). Control of

microtubule dynamics by Stu2p is essential for spindle orientation and metaphase chromosome alignment in yeast. Mol. Biol. Cell *12*, 2870–2880.

Li, Y.Y., Yeh, E. Hays, T., and Bloom, K. (1993). Disruption of mitotic spindle orientation in a yeast dynein mutant. Proc. Natl. Acad. Sci. USA *90*, 10096–10100.

Manning, B.D., Barrett, J.G., Wallace, J.A., Granok, H., and Snyder, M. (1999). Differential regulation of the Kar3 kinesin regulated protein by two associated proteins, Cik1p and Vik1p. J. Cell Biol. *144*, 1219–1233.

Meluh, P.B., and Rose, M.D. (1990). Kar3, a kinesin-related gene required for yeast nuclear fusion. Cell *60*, 1029–1041.

Miller, R.K., Cheng, S.C., and Rose, M.D. (2000). Bim1p/Yeb1p mediates the Kar9p-dependent cortical attachment of cytoplasmic microtubules. Mol. Biol. Cell *11*, 2949–2959.

Miller, R.K., and Rose, M.D. (1998). Kar9p is a novel cortical protein required for cytoplasmic microtubule orientation in yeast. J. Cell Biol. *140*, 377–390.

Moens, P.B., and Rapport, E. (1971). Spindles, spindle plaques, and meiosis in the yeast *Saccharomyces cerevisiae*. J. Cell Biol. *50*, 344–361.

Murphy, S.M., Urbani, L., and Stearns, T. (1998). The mammalian gamma-tubulin complex contains homologues of the yeast spindle pole body components spc97p and spc98p. J. Cell Biol. *141*, 663–674.

Nguyen, T., Vinh, D.B.N., Crawford, D.K., and Davis, T.N. (1998). A genetic analysis of interactions with Spc110p reveals distinct functions of Spc97p and Spc98p components of the yeast gamma-tubulin complex. Mol. Biol. Cell *9*, 2201–2216.

Page, B.D., and Snyder, M. (1992). CIK1: a developmentally regulated spindle pole body-associated protein important for micortubule functions in *Saccharomyces cerevisiae*. Genes Dev. *6*, 1414–1429.

Palmer, R.E., Sullivan, D.S., Huffaker, T., and Koshland, D. (1992). Role of astral microtubules and actin in spindle orientation and migration in the budding yeast. *Saccharomyces cerevisiae*. J. Cell Biol. *119*, 583–593.

Pereira, G., Gruenenberg, U., Knop, M., and Schiebel, E. (1999). Interaction of the yeast gamma-tubulin complex-binding protein Spc72p with Kar1p is essential for microtubule function during karyogamy. EMBO J. *18*, 4180–4195.

Piel, M., Meyer, P., Khodjakov, A., Rieder, C.L., and Bornens, M. (2000). The respective contributions of the mother and daughter centrioles to centrosome activity and behavior in vertebrate cells. J. Cell Biol. *149*, 317–330.

Rout, M.P., and Kilmartin, J.V. (1990). Components of the yeast spindle and spindle pole body. J. Cell Biol. *111*, 1913–1927.

Sambrook, J., Fritsch, E.F., and Maniatis, T. (1989). Molecular Cloning: A Laboratory Manual, 2nd ed., Cold Spring Harbor, NY: Cold Spring Harbor Laboratory.

Saunders, W., Hornack, D., Lengyel, V., and Deng, C. (1997). The *Saccharomyces cerevisiae* kinesin-related motor Kar3p acts at preanaphase spindle poles to limit the number and length of cytoplasmic microtubules. J. Cell Biol. *137*, 417–431.

Schaerer, F., Morgan, G., Giddings, T., Winey, M., and Philippsen, P. (2001). Cnm67p is a spacer of the *Saccharomyces cerevisiae* spindle pole body outer plaque. Mol. Biol. Cell *12*, 2519–2533.

Schiestl, R.H., and Gietz, R.D. (1989). High efficiency transformation of intact yeast cells using single stranded nucleic acids as a carrier. Curr. Genet. *16*, 339–346.

Segal, M., Bloom, K., and Reed, S.I. (2000). Bud6 directs sequential microtubule interactions with the bud tip, and bud neck during spindle morphogenesis in *Saccharomyces cerevisiae*. Mol. Biol. Cell *11*, 3689–3702.

Shaw, S.L., Yeh, E., Maddox, P., Salmon, E.D., and Bloom, K. (1997). Astral microtubule dynamics in yeast: a microtubule-based searching mechanism for spindle orientation and nuclear migration into the bud. J. Cell Biol. *139*, 985–994.

Souès, S., and Adams, I.R. (1998). SPC72: a spindle pole component required for spindle orientation in the yeast *Saccharomyces cerevisiae*. J. Cell Sci. *111*, 2809–2818.

Spang, A., Geissler, S., Grein, K., and Schiebel, E. (1996). γ-Tubulin-like Tub4p of *Saccharomyces cerevisiae* is associated with the spindle pole body substructures that organize microtubules and is required for mitotic spindle formation. J. Cell Biol. *134*, 429–441.

Straight, A.F., Marshall, W.F., Sedat, J.W., and Murray, A.W. (1997). Mitosis in living yeast: anaphase A but not metaphase plate. Science *277*, 574–578.

Straight, A.F., Sedat, J.W., and Murray, A.W. (1998). Time-lapse microscopy reveals unique roles for kinesins during anaphase in budding yeast. J. Cell Biol. *143*, 687–694.

Sullivan, D.S., and Huffaker, T.C. (1992). Astral microtubules are not required for anaphase B in *Saccharomyces cerevisiae*. J. Cell Biol. *119*, 379–388.

Tirnauer, J.S., O'Toole, E., Berrueta, L., Bierer, B.E., and Pellman, D. (1999). Yeast Bim1p promotes the G1-spcific dynamics of microtubules. J. Cell Biol. *145*, 993–1007.

Wach, A., Brachat, A., Alberti-Segui, C., Rebischung, C., and Philippsen, P. (1997). Heterologous HIS3 marker and GFP reporter modules for PCR-targeting in *Saccharomyces cerevisiae*. Yeast *13*, 1065–1075.

Wach, A., Brachat, A., Pöhlmann, R., and Philippsen, P. (1994). New heterologous modules for classical or PCR-based gene disruptions in *Saccharomyces cerevisiae*. Yeast *10*, 1793–1808.

Wang, P.J., and Huffaker, T.C. (1997). Stu2p: a microtubule-binding protein that is an essential component of the yeast spindle pole body. J. Cell Biol. *139*, 1271–1280.

Yeh, E., Yang, C., Chin, E., Maddox, P., Salmon, E.D., Lew, D.J., and Bloom, K. (2000). Dynamic positioning of mitotic spindles in yeast: role of microtubule motors and cortical determinants. Mol. Biol. Cell *11*, 3949–3961.

Yin, H., Pruyne, D., Huffaker, T.C., and Bretscher, A. (2000). Myosin V orientates the mitotic spindle in yeast. Nature *406*, 1013–1015.